THE JOURNAL OF BIOLOGICAL CHEMISTRY
Vol. 273, No. 22, Issue of May 29, pp. 13819–13827, 1998
Printed in U.S.A.

Alternative Intracellular Routing of ErbB Receptors May Determine Signaling Potency*

(Received for publication, October 3, 1997, and in revised form, February 23, 1998)

Hadassa Waterman‡, Ilana Sabanai§, Benjamin Geiger§, and Yosef Yarden‡¶

From the Departments of ‡Biological Regulation and §Molecular Cell Biology, The Weizmann Institute of Science, Rehovot 76100, Israel

The ErbB signaling module consists of four receptor tyrosine kinases and several dozen ligands that activate specific homo- and heterodimeric complexes of ErbB proteins. Combinatorial ligand/receptor/effector interactions allow large potential for signal diversification. Here we addressed the possibility that turn-off mechanisms enhance the diversification potential. Concentrating on ErbB-1 and two of its ligands, epidermal growth factor (EGF) and transforming growth factor α (TGF-α), and the Neu differentiation factor (NDF/neuregulin) and one of its receptors, ErbB-3, we show that ligand binding variably accelerates endocytosis of the respective ligand-receptor complex. However, unlike the EGF-activated ErbB-1, which is destined primarily to degradation in lysosomes, NDF and TGF-α direct their receptors to recycling, probably because these ligands dissociate from their receptors earlier along the endocytic pathway. In the case of NDF, structural, as well as biochemical, analyses imply that ligand degradation occurs at a relatively late endosomal stage. Attenuation of receptor down-regulation by this mechanism apparently confers to both NDF and TGF-α more potent and prolonged signaling activity. In conclusion, alternative endocytic trafficking of ligand-ErbB complexes may tune and diversify signal transduction by EGF family ligands.

The ErbB/HER family of receptor tyrosine kinases is representative of several other groups of highly homologous receptors sharing growth factors as their ligands (1). Whereas only one ErbB homolog exists in invertebrates, such as flies and worms, four receptors are present in mammals, and they bind to multiple growth factor molecules through an epidermal growth factor (EGF)[1] motif. The variety of receptors and ligands is thought to contribute to the diversification potential of the ErbB signaling network (reviewed in Ref. 2). Three levels of signal diversification may be proposed. First, each ligand molecule is apparently bivalent; the high affinity binding site binds to a "primary receptor," whereas a low affinity site, whose specificity is broad, allows selective recruitment of ErbB molecules into dimeric receptor structures, leading to effective signaling (3). Second, at the receptor level, 10 distinct homo- and heterodimeric complexes may be formed in a ligand-specific order of preference. Yet, the most divergent level of the signaling mechanism appears to be postreceptor; through their various autophosphorylation sites, dimeric receptor complexes engage specific sets of cytoplasmic signaling proteins sharing a phosphotyrosine binding motif, usually a Src homology 2 domain (4).

Despite the remarkably large repertoire of signaling proteins that become physically associated with specific ErbB dimers, only a few have been shown to be strictly specific. Examples include the phosphatidylinositol 3′-kinase, an enzyme that selectively binds to ErbB-3-containing dimers (5), and phospholipase Cγ, a specific target of ErbB-1 (6) and ErbB-2 (7). Moreover, signaling pathways stimulated by all ErbB combinations feed into the mitogen-activated protein kinase (MAP kinase) pathway (8), resulting in a surprisingly uniform pattern of signaling, which is shared by the invertebrate versions of ErbB proteins (9). Nevertheless, unlike the shared rapid coupling to MAP kinases, the kinetics of MAP kinase inactivation, a critical parameter in determining signal outcome (10), differ according to the identity of the stimulating receptor. Especially important is the engagement of ErbB-2, a ligandless protein that delays inactivation of ErbB signals (11), and ErbB-3, a kinase-defective receptor whose activation depends on the presence of a co-receptor (8, 12). Thus, the inactivation phase of ErbB signaling may be critical for determination of the duration and potency of cell activation by EGF family growth factors.

Whereas the major events involved in ErbB activation are fairly well understood, the inactivation phase is still poorly characterized. Several lines of evidence, however, suggest that turn-off mechanisms may be as important for signal diversification as is the stimulatory process. An obvious candidate is the interaction of ligand-occupied receptors with tyrosine-specific phosphatases (13). Cbl is another example; this cytoplasmic adaptor protein, whose ortholog in *Caenorhabditis elegans* negatively regulates ErbB signaling (14), associates with ErbB-1 but not with ErbB-3 or with ErbB-4 (15). The third mechanism of receptor inactivation involves ligand-induced down-regulation of the number of surface receptors. This fairly complex regulatory process is mediated by rapid endocytosis of ligand-receptor complexes, and their variable delivery into cytoplasmic compartments (for review see Ref. 16). Unlike receptors for nutrients such as transferrin and lipoproteins, efficient internalization of growth factor receptors through coated pits requires ligand binding. In addition, a more significant fraction of the endocytosed signaling receptors escapes recycling and is sorted to degradation in lysosomes. Apparently, a fine balance between receptor recycling and lysosomal targeting exists in cells, yet its molecular details are still poorly understood. For

* This work was supported by the Susan G. Komen Breast Cancer Foundation; NCI, National Institutes of Health Grant CA72981; and the Israel Science Foundation. The costs of publication of this article were defrayed in part by the payment of page charges. This article must therefore be hereby marked "*advertisement*" in accordance with 18 U.S.C. Section 1734 solely to indicate this fact.

¶ To whom correspondence should be addressed: Dept. of Biological Regulation, The Weizmann Institute of Science, Rehovot 76100, Israel. Tel.: 972-8-9343974; Fax: 972-8-9344125; E-mail: liyarden@weizmann.weizmann.ac.il.

[1] The abbreviations used are: EGF, epidermal growth factor; CHO, Chinese hamster ovary, MTT, 3-(4,5-dimethylthiazol-2-yl)-2,5-diphenyl tetrazolium bromide; NDF, Neu differentiation factor; TGF-α, transforming growth factor α; MAP, mitogen-activated protein.

example, specific domains of ErbB-1 are necessary for lysosomal targeting (17), and certain cytoplasmic proteins, such as phosphatidylinositol 3′-kinase, are probably involved in the selective sorting of internalized receptors (18). Another critical parameter is the pH sensitivity of ligand/receptor interactions; ligands, such as EGF, whose interaction is relatively resistant to mildly acidic pH, target ErbB-1 to lysosomes, whereas transforming growth factor α (TGF-α) and other ligands that readily dissociate due to the mildly acidic endosomal pH cause receptor recycling (19). Despite the open questions, it seems clear that endocytosis and lysosomal targeting critically attenuate signaling by growth factors (20, 21).

Recent reports suggest that alternative intracellular routing of ErbB proteins and their ligands may contribute to diversification of signal transduction (8, 22). In contrast to the rapid internalization of ErbB-1 and its ligand, EGF, retarded endocytosis of the three other members of the ErbB family has been observed. In this paper, we have investigated the mechanism underlying differential receptor trafficking by ErbB ligands. We have found that an ErbB-3-specific ligand, the Neu differentiation factor (NDF/neuregulin), undergoes slow endocytosis that is followed by receptor recycling to the plasma membrane. By contrast, most of the EGF-stimulated ErbB-1 molecules are destined to lysosomal degradation. Due to the consequent clearance of ErbB-1 molecules, but not ErbB-3 molecules, from the cell surface, the mitogenic signal evoked by EGF is less potent than the NDF signal. This phenomenon, however, depends also on the nature of the ligand, since another ErbB-1 ligand, TGF-α, undergoes rapid endocytosis but nevertheless induces receptor recycling with only limited receptor down-regulation. Consistently, the mitogenic activity of this ligand is superior to that of EGF, reinforcing a role for ErbB routing in tuning of mitogenic signals.

EXPERIMENTAL PROCEDURES

Materials, Buffers, and Antibodies—A recombinant form of NDF-$\beta1_{177–246}$ was prepared by Amgen (Thousand Oaks, CA). Human recombinant EGF and TGF-α were purchased from Sigma. Radioactive materials were purchased from Amersham Pharmacia Biotech. IODO-GEN was from Pierce. A monoclonal antibody to ErbB-3 was generated in our laboratory (23). The ErbB-1-specific monoclonal antibody 528 was a gift from John Mendelsohn (M. D. Anderson Cancer Center). The monoclonal antibody to the active form of MAP kinase (doubly phosphorylated on both tyrosine and threonine residues of the TEY motif (24)) was a gift from Rony Seger (Weizmann Institute, Rehovot, Israel). Binding buffer contained Dulbecco's modified Eagle's medium with 0.5% bovine serum albumin and 20 mM HEPES. HNTG buffer contained 20 mM HEPES (pH 7.5), 150 mM NaCl, 0.1% Triton X-100, and 10% glycerol. Solubilization buffer contained 50 mM Tris-HCl, pH 7.5, 150 mM NaCl, 10% glycerol, 1% Nonidet P-40, 1.5 mM EGTA, 2 mM sodium orthovanadate, 1 mM phenylmethylsulfonyl fluoride, aprotinin (0.15 trypsin inhibitor unit/ml), and 10 μg/ml leupeptin. Biotin-X-NHS was from Calbiochem. Colloidal gold sols (10-nm diameter) were from British Biocell International. All other chemicals were purchased from Sigma, unless otherwise indicated.

Cell Lines—The Chinese hamster ovary (CHO) cell lines expressing the various ErbB proteins or a deletion mutant of ErbB-3 were described previously (25). The ErbB-3 QQGFF insertion mutant was generated by oligonucleotide-directed mutagenesis using T7-DNA polymerase (26). The cDNA of *erbB-3* was subcloned into the pCDNA3 expression vector containing an F1 origin of replication, and the mutation was introduced by using the primer 5′-GGAGCAGGAGTTAGAAAAAGCCCTGTTGCGTTCTCTGGG-3′ and the purified single-stranded DNA as a template. Cells were cultured in Dulbecco's modified Eagle's medium/F-12 medium supplemented with antibiotics and 10% heat-inactivated bovine serum. For immunoprecipitation and immunoblotting experiments, cells were grown to 90% confluence. Sublines derived from the 32D murine hematopoietic progenitor cell line and expressing various ErbB proteins have been previously described (8). Cells were grown in RPMI 1640 medium supplemented with antibiotics, 10% heat-inactivated fetal bovine serum, and 0.1% medium that was conditioned by an interleukin-3-producing cell line (27).

Radiolabeling of Ligands and Ligand Binding Analyses—Human recombinant EGF, TGF-α, and human recombinant NDF-$\beta1_{177–246}$ were labeled with IODO-GEN (Pierce) as described (3). For binding assays, monolayers of the indicated cell lines in 24-well dishes were washed once with binding buffer and then incubated for 2 h at 4 °C with 10 ng/ml ^{125}I-labeled NDF-$\beta1_{177–246}$, ^{125}I-EGF, or TGF-α. The cells were washed three times with ice-cold binding buffer. Labeled cells were lysed for 15 min at 37 °C in 0.5 ml of 0.1 N NaOH solution containing 0.1% SDS, and the radioactivity was determined. Nonspecific binding was calculated by subtracting the binding of radiolabeled ligands to CHO cells or by performing the binding assays in the presence of a 100-fold excess of unlabeled ligand.

Ligand Internalization Assay—Cells cultured in 24-well plates were washed with binding buffer and then incubated for 2 h at 4 °C in the presence of radiolabeled NDF or EGF (each at 10 ng/ml). To allow ligand internalization, the cells were transferred to 37 °C and incubated for various periods of time. The cells were then put on ice and washed twice with binding buffer, and cellular distribution of the radiolabeled ligand was determined by using a 7-min-long incubation in 0.5 ml solution of 150 mM acetic acid (pH 2.7), containing 150 mM NaCl. The released ligand was considered as cell surface-associated ligand (28). The remaining radioactivity was solubilized in 100 mM NaOH solution containing 0.1% SDS that was considered as internalized ligand.

Receptor Down-regulation Assay—Ligand-induced receptor down-regulation was measured as follows. Cells grown in 24-well plates were incubated at 37 °C for up to 2.5 h without or with 250 ng/ml ligand in binding buffer and then rinsed with cold binding buffer. Surface-bound growth factor was removed by using a low pH acetic acid wash. The number of ligand binding sites on the cell surface was then determined by incubating cells at 4 °C with the corresponding radiolabeled ligand for at least 1 h.

Electron Microscopy—Coupling of EGF and NDF to gold colloids (10-nm diameter) was performed by using a standard protocol provided by the manufacturer. Cellular uptake of colloidal gold-labeled ligands was performed as follows. Cells grown in 24-well plates were rinsed twice with binding buffer at 4 °C and then incubated in the same buffer containing 1:10 dilution of either NDF- or EGF-colloidal gold for 45 min at 4 °C. The cells were then warmed to 37 °C and incubated for various time intervals in the continuous presence of the ligand. At the end of incubation at 37 °C, cells were rinsed twice with binding buffer and fixed for 24 h with Karnovsky's fixative (3% formaldehyde, 2% glutaraldehyde, and 5 mM $CaCl_2$ in 100 mM cacodylate buffer, pH 7.4) at room temperature and 10 h at 4 °C. Lighter fixation was then carried out with a mixture of 3% formaldehyde and 0.1% glutaraldehyde in the same buffer. Tissues were impregnated in 100 mM cacodylate buffer, with 2.3 M sucrose, pH 7.4. The samples were quickly frozen in liquid nitrogen, and ultrathin sections (500–1000 Å) were cut at −115 °C using a Reichert-Jung FS-4D ultracryomicrotome. The sections were recovered from the knife in a 2.3 M sucrose droplet according to the method of Tokuyasu and Singer (29) and transferred to Formvar-coated 300-mesh grids. The grids were floated on water in a Petri dish at 4 °C. The duration of the water rinse was between 1 and 16 h, without any appreciable difference in the resulting ultrastructure. The sections were then processed for methyl-cellulose mounting according to a modification of the above mentioned protocol.

Cell Proliferation Assay—Cells were washed free of interleukin-3, resuspended in RPMI 1640 medium at 5×10^5 cells/ml, and treated without or with EGF, TGF-α, or NDF at various concentrations for dose response experiments. Cell survival was determined by using the [3-(4,5-dimethylthiazol-2-yl)-2,5-diphenyl tetrazolium bromide (MTT) assay, which determines mitochondrial activity in living cells (30). MTT (0.1 mg/ml) was incubated with the analyzed cells for 2 h at 37 °C. Living cells can transform the tetrazolium ring into dark blue formazan crystals that can be quantified by reading the optical density at 540–630 nm after lysis of the cells with acidic isopropyl alcohol.

Cell Surface Biotinylation—Monolayers of CHO cells grown in 10-cm dishes were washed three times with ice-cold phosphate-buffered saline and then incubated with 0.5 mg/ml of a water-soluble Biotin-X-NHS (Calbiochem) dissolved in borate buffer (10 mM boric acid, 150 mM NaCl, pH 8.0) for 45 min at 4 °C. Coupling of biotin was blocked by extensive washes with a solution of 15 mM glycine in phosphate-buffered saline. Cells were then treated with a growth factor (250 ng/ml) for different time intervals at 37 °C. To evaluate the amounts of cell surface receptors, the cells were subjected to immunoprecipitation and gel electrophoresis. Visualization of the biotinylated proteins was performed by probing the nitrocellulose membranes with horseradish peroxidase-conjugated streptavidin (Amersham Pharmacia Biotech) and developed

with an enhanced chemiluminescence reagent (Amersham Pharmacia Biotech).

Lysate Preparation and Immunoprecipitation—After treatment with growth factors, cells were scrapped, pelleted by centrifugation, and solubilized in solubilization buffer. Lysates were cleared by centrifugation (10,000 × *g*, 10 min). For direct electrophoretic analysis, boiling gel sample buffer was added to cell lysates. For other experiments, lysates were first subjected to immunoprecipitation with anti-receptor monoclonal antibodies that were precoupled to rabbit-anti-mouse immunoglobulin G and then to protein A-Sepharose. The proteins in the lysate supernatant were immunoprecipitated with aliquots of the protein A-Sepharose-antibody complex for 2 h at 4 °C. The immunoprecipitates were washed three times with HNTG, resolved by SDS-polyacrylamide gel electrophoresis through 7.5% gels, and electrophoretically transferred to nitrocellulose membranes. Membranes were blocked for 2 h in TBST buffer (0.02 M Tris-HCl, pH 7.5, 0.15 M NaCl, and 0.05% Tween 20) containing 0.1% milk, blotted with 1 μg/ml primary antibodies for 2 h, followed by 0.5 μg/ml secondary antibody linked to horseradish peroxidase. Immunoreactive bands were detected with the ECL (enhanced chemiluminescence) reagent (Amersham Pharmacia Biotech).

Analysis of Growth Factor Degradation—Conditioned media containing radiolabeled ligands were assayed by the addition of cold trichloroacetic acid (10% final concentration). Samples were precipitated after 1 h at 2 °C by centrifugation for 15 min at 4 °C. Radioactivity present in the supernatants (trichloroacetic acid-soluble fraction) and pellets (trichloroacetic acid-insoluble fraction) was determined.

RESULTS

NDF and EGF Receptors Are Differentially Endocytosed and Metabolized following Ligand Binding—It has been previously reported that the rates of ligand-induced internalization of NDF receptors are significantly slower than the rate of EGF-driven endocytosis of ErbB-1 (8, 22). We used a series of CHO cells (25), which share landmarks with many ErbB-expressing epithelial and fibroblastic cells, to address the mechanism underlying differential endocytosis of ErbB proteins. Comparative analysis revealed that CHO cells ectopically expressing ErbB-1 (denoted CB1 cells) internalized radiolabeled EGF at a higher rate than the kinetics of endocytosis of surface-bound NDF into cells expressing ErbB-3 (CB3 cells) or ErbB-4 (CB4 cells, Fig. 1*A*). Two lines of evidence indicated that this difference is receptor-specific rather than ligand-specific. First, internalization of EGF by cells expressing a chimeric receptor, denoted NEC, in which the extracellular and intracellular domains are derived from ErbB-1 and ErbB-2, respectively (31), was relatively slow, in accordance with a previous report (32). Second, the rate of internalization of another ErbB-1 ligand, namely TGF-α, was comparable with that of EGF (Fig. 1*A*). These results are consistent with previous reports (8, 22, 33), and they imply that the differences in cellular uptake of NDF and EGF are independent of cell type or ligand identity.

To gain insight into the mechanism of the relatively slow internalization of NDF, we concentrated on one of its receptors, ErbB-3, and analyzed its fate in the presence or absence of the ligand. For comparison, we used ErbB-1 and two of its ligands, EGF and TGF-α, because differences in cellular routing of these growth factors, when complexed to ErbB-1, have previously been noted (34). Labeling of cell surface receptor molecules with biotin and subsequent immunoprecipitation analysis revealed that ErbB-3 underwent a constitutively rapid down-regulation, which was only moderately enhanced by NDF (Fig. 1*C*). By contrast, ErbB-1 displayed a relatively long membrane residence, and it was rapidly cleared from the cell surface after binding of EGF (Fig. 1*B*). It is noteworthy that analysis of a chimeric ErbB-3 molecule, whose extracellular domain was derived from ErbB-1, detected a very small effect of the ligand on the half-life of the metabolically labeled ErbB-3 chimera (22). A third pattern of down-regulation was displayed by the TGF-α-activated ErbB-1. This ligand exerted no detectable effect on surface ErbB-1 (Fig. 1*B*). We concluded that the turnover rates of surface-exposed ErbB-3 and ErbB-1 molecules differ even in the absence of a ligand. However, the extent of ligand-induced down-regulation depends on ligand identity, as exemplified by the comparison between EGF and TGF-α.

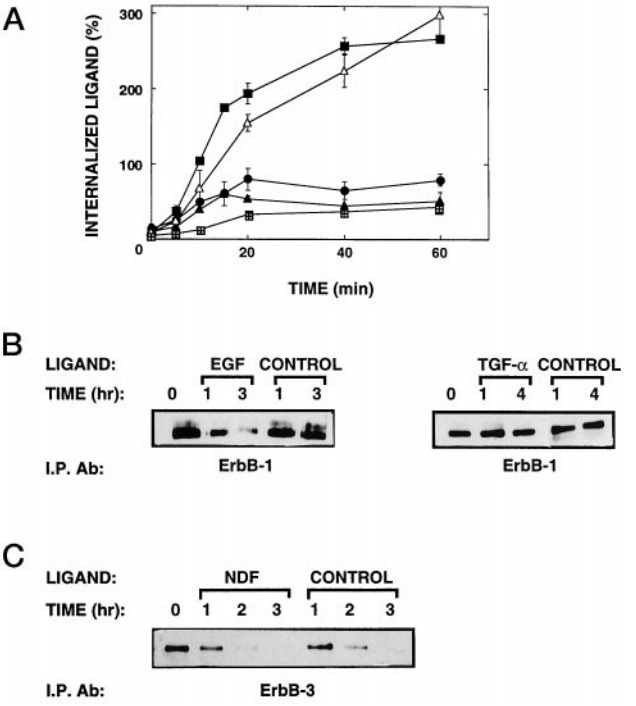

FIG. 1. **Differential internalization of ErbB proteins and their ligands.** *A*, ligand internalization. Cell monolayers were treated for 2 h at 4 °C with various radiolabeled ligands (each at 10 ng/ml) and then transferred to 37 °C for the indicated periods of time. At the end of incubation, cells were rinsed twice with binding buffer and then treated with a low pH stripping buffer that removes surface-bound ligand. The fraction of the acid-inaccessible internalized ligand is presented as the percentage of intracellular radioactivity at each time point relative to the total cell-associated radioactivity prior to transfer to 37 °C. Because at the temperature shift the unbound ligand was not removed from the medium, its association with cells increased above 100%. The following ligands and sublines of CHO cells were used. EGF (*closed squares*) and TGF-α (*open triangles*) were tested with cells singly expressing ErbB-1 (CB1 cells). In a similar way, we tested NDF endocytosis by ErbB-3-expressing cells (CB3 cells, *closed circles*), or ErbB-4-expressing cells (CB4 cells, *closed triangles*) and EGF internalization into cells expressing a chimeric ErbB-1 (extracellular portion) fused to the transmembrane and cytoplasmic part of ErbB-2 (NEC cells, *crossed squares*). Each data point represents the average and ranges (*bars*) of duplicate measurements from which the amount of nonspecifically bound ligand was subtracted. The experiment was repeated three times. *B* and *C*, receptor degradation. CB1 (*B*) and CB3 (*C*) cells were surface-labeled by a 40-min-long incubation with NHS-biotin (0.5 mg/ml) at 4 °C. Labeled cells were washed with a glycine-containing solution to block the residual reactive compound and then incubated for the indicated time intervals at 37 °C without (*CONTROL*) or with the indicated ligands (each at 250 ng/ml). Whole cell lysates were then prepared, and the indicated ErbB proteins were immunoprecipitated (*I.P.*). Following separation of the immune complexes by gel electrophoresis and electrotransfer to nitrocellulose filters the filters were probed with horseradish peroxidase-labeled avidin. Only the 180-kilodalton region of the blots is shown.

To further follow the differences in receptor down-regulation, we used a ligand binding assay as an alternative measure of the decrease in the number of cell surface receptors following stimulation with a growth factor. The ability of EGF, TGF-α, and NDF to down-regulate ErbB receptors was examined in the absence or presence of monensin, a carboxylic ionophore that disrupts intracellular traffic and receptor recycling (35). As shown in Fig. 2, in the absence of the inhibitor, ErbB-1 molecules were down-regulated within 30 min by approximately 80%, while at this time point both NDF and TGF-α caused the disappearance of only a quarter of their respective receptors.

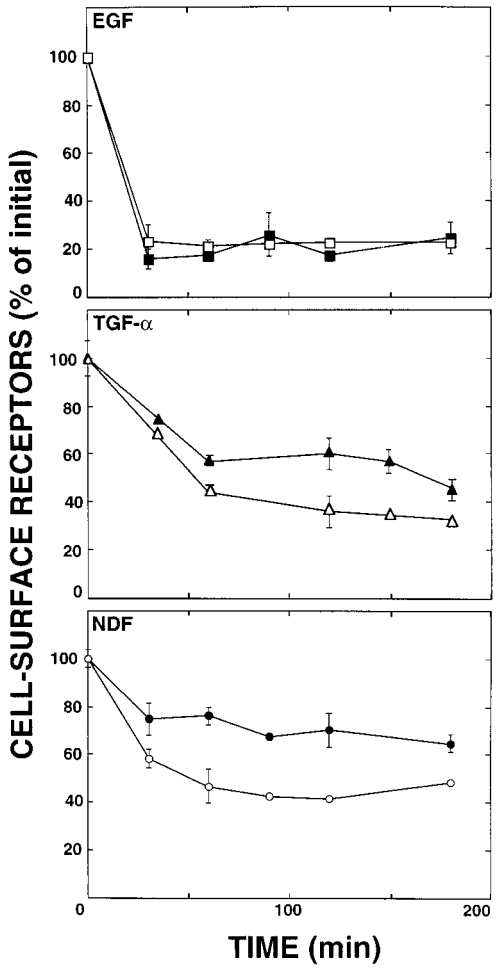

FIG. 2. **Ligand-dependent down-regulation of ErbB-1 and ErbB-3 and the effect of monensin.** CB1 (*A* and *B*) and CB3 (*C*) cells were grown to 80% confluence in 24-well plates, washed with binding buffer, and incubated at 37 °C for the indicated periods of time with the following ligands (each at 250 ng/ml): EGF (*squares*), TGF-α (*triangles*), or NDF (*circles*). Sister cultures were similarly treated, except that monensin (50 μM) was added to the medium (*open symbols*). Thereafter, monolayers were rinsed twice with binding buffer, followed by a 7-min-long incubation with a low pH stripping buffer, to remove surface-bound ligands. The level of surface receptors, relative to the initial number of ligand binding sites, was then determined by incubating the cells for 1.5 h at 4 °C with the corresponding radiolabeled ligand. The results are expressed as the average fraction (and range, *bars*) of original binding sites that remained on the cell surface after exposure to the nonlabeled ligand at 37 °C.

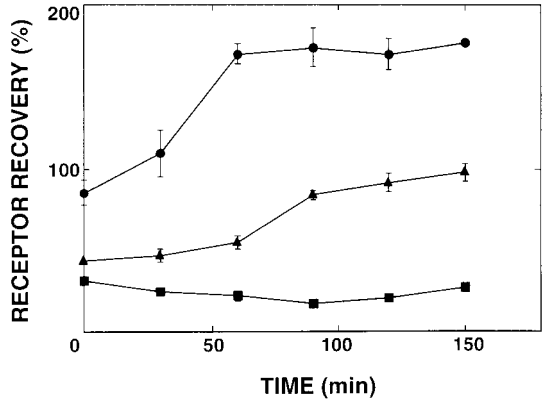

FIG. 3. **Reappearance of ErbB proteins at the cell surface after receptor down-regulation.** CB1 cells were exposed to either EGF (*squares*) or TGF-α (*triangles*, each at 250 ng/ml) for 2 h at 37 °C. Likewise, CB3 cells were exposed to NDF (*circles*). Cell-bound ligand was then removed at 4 °C by using an acidic pH buffer, and cells were transferred back to 37 °C to allow receptor recovery for the indicated time intervals. Surface-associated ligand binding sites were then determined at 4 °C by using a radiolabeled ligand binding assay, as described under "Experimental Procedures." The results are presented as the average and range (*bars*) of the number of binding sites at each time point, relative to the original receptor level. Note that initial receptor levels differ, due to differences in the extent of down-regulation prior to the recovery period.

Inhibition of receptor recycling, however, increased the extent of down-regulation by NDF, as well as by TGF-α, but the drug was ineffective on the EGF-induced down-regulation of ErbB-1 (Fig. 2). In analogy to previous models of TGF-α-induced down-regulation (34, 36), one possible interpretation of our results is as follows. NDF, as well as TGF-α, targets its receptor to a recycling pathway, whereas the EGF-bound ErbB-1 is destined primarily to intracellular degradation. If correct, this model predicts that receptor recovery following down-regulation will be rapid in the case of the recycling-inducing ligands (*i.e.* NDF and TGF-α), but only slow recovery of ErbB-1 may be expected after stimulation with EGF. In order to examine this prediction, receptors were down-regulated in the presence of high ligand concentrations, and the cells were subsequently acid-washed to remove surface-bound ligand molecules. Later, treated cells were transferred to 37 °C to allow receptor recovery at the cell surface. Recovery was detected by rebinding of a labeled ligand. In line with the proposed model, rapid recovery followed down-regulation by NDF or TGF-α, but practically no reappearance of binding sites was coupled to the EGF-induced down-regulation of ErbB-1 (Fig. 3). The extra recovery displayed by ErbB-3 is surprising and may be due to an intracellular pool of ErbB-3, whose existence is consistent with the short half-life of this receptor (Fig. 1*C*), and its mostly cytoplasmic, rather than cell membrane, localization as revealed by immunostaining (37).

NDF and EGF Undergo Differential Intracellular Metabolism, Probably Due to Distinct pH Sensitivity of Ligand/Receptor Interactions—Mutations in several types of receptors, including the low density lipoprotein receptor (38) and the insulin receptor (39), accelerate ligand degradation by stabilizing the ligand-receptor complex at the low pH (pH ≲6.2) of endosomes (40). Likewise, the pH sensitivity of ErbB-1/ligand interactions apparently affects the balance between recycling and degradation of EGF family ligands (19). To determine whether differential dissociation of NDF, EGF, and TGF-α can account for alternative routing of their receptors, we tested the stability of the corresponding ligand-receptor complexes at various pH conditions. As is evident from Fig. 4, NDF, like TGF-α, displayed higher pH sensitivity than EGF at the relevant range of pH values, supporting a model attributing recycling of ErbB-3 to NDF-ErbB-3 dissociation in early endosomes.

Following receptor-mediated internalization, EGF was shown to be degraded in lysosomes, and the degradation products were released into the medium (16). In order to study the sorting of NDF after its uptake by ErbB-3, we incubated cells in the presence of the radiolabeled ligand at 20 °C, a temperature that allows internalization but not degradation. The ligand was then removed, and the preloaded cells were chased by warming to 37 °C. This allowed a sensitive, time-synchronized, test of the fate of the internalized ligand (41). The results presented in Fig. 5 show that all three ligands, NDF, TGF-α, and EGF, underwent significant and comparable degradation upon transfer to 37 °C. To unravel possible differences, we used chloroquine, a drug known to inhibit degradation in both endosomal (prelysosomal) and lysosomal compartments, and leupeptin, a tripeptide whose inhibitory action is specific to lysosomes (42, 43). The drugs were preincubated with cells prior to the tem-

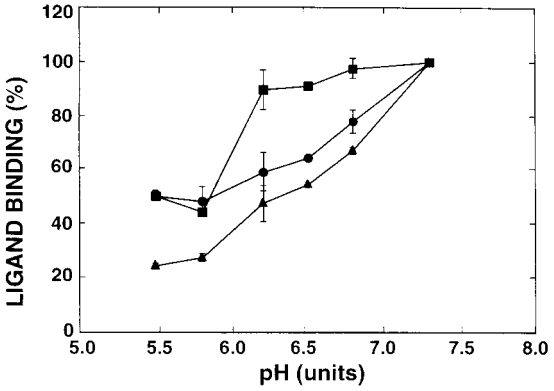

FIG. 4. **pH dependence of ligand binding to ErbB proteins.** CB1 cells were incubated for 2 h at 4 °C with either ^{125}I-EGF (*squares*) or ^{125}I-TGF-α (*triangles*) in binding solutions whose pH was adjusted at different values, as indicated. Similarly, CB3 cells were incubated with radiolabeled NDF (*circles*; each ligand was used at 10 ng/ml). At the end of the incubation period, cells were lysed, and their radioactivity was determined. Nonspecific ligand binding at each condition was assayed by using a large excess of the corresponding ligand. The results are presented as an average and range (*bars*) of a duplicate determination of the specific ligand binding relative to the amount of ligand that bound at pH 7.5. The experiment was repeated three times.

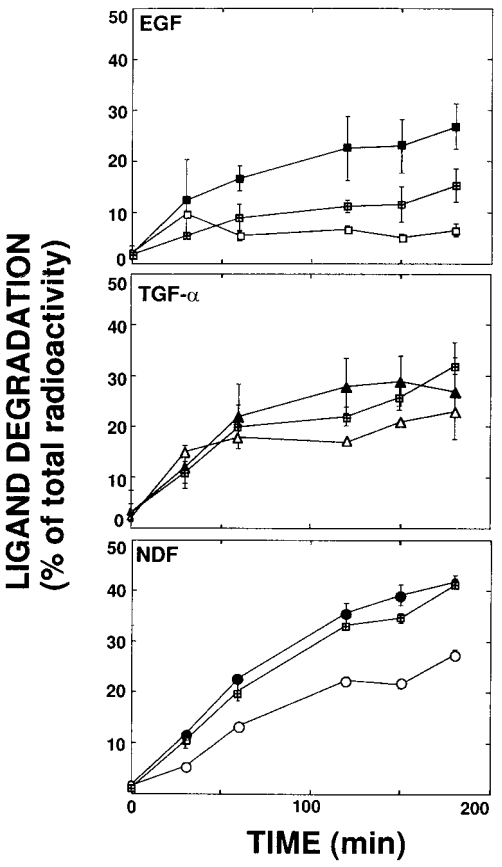

FIG. 5. **Kinetics of ErbB-mediated ligand degradation.** Monolayers of CB1 (*two upper panels*) or CB3 cells (*lower panel*) were incubated for 1 h at 20 °C with either EGF (*closed squares*), TGF-α (*closed triangles*), or NDF (*closed circles*), in order to allow intracellular accumulation of the respective radioactive ligand with only limited degradation. Thereafter, cells were washed in binding buffer and maintained at 37 °C for the indicated time intervals. Media were then collected, and cells were solubilized. The fraction of acid-soluble (degraded) ligand in the medium was then determined by counting the trichloroacetic acid-precipitable radioactivity in the medium and the total cell-associated radioactivity. Sister monolayers were similarly treated, except that incubation was performed in the presence of leupeptin (1 mM, *crossed squares*), or chloroquine (0.1 mM, *open symbols*). The results are expressed as the average percentage of trichloroacetic acid-soluble radioactivity, relative to the sum of cell-associated and medium-released radioactivity. The experiment was performed in duplicate and repeated twice.

perature shift and ligand degradation assays. Surprisingly, in contrast to the complete inhibition of EGF degradation by chloroquine, this drug only partially inhibited degradation of NDF and TGF-α (Fig. 5). On the other hand, leupeptin exerted no significant inhibition of NDF and TGF-α, but proteolysis of EGF was partially blocked. In conclusion, although ErbB-3 is recycled, its ligand, NDF, apparently undergoes intracellular degradation in a nonlysosomal compartment that is leupeptin-insensitive but is partially inhibited by chloroquine. This characteristic is shared with the TGF-α-driven ErbB-1, which like ErbB-3, is diverted to recycling.

Subcellular Distribution of Internalized NDF—Endocytosed molecules are first delivered to early endosomes, which are tubular and vesicular membrane structures often connected to networks and located at the cell periphery. EGF and its receptor can be detected in this compartment within 2–5 min of internalization onset (44). After 10–15 min, EGF-occupied ErbB-1 molecules begin to accumulate in large tubular-vesicular endosomes, located mainly around the nucleus. EGF and ErbB-1 become detectable within lysosomes after 30–60 min of internalization, but they are retained in these compartments for several hours. To follow the subcellular distribution of internalized NDF, in comparison with EGF, we examined the distribution of colloidal gold-labeled NDF and EGF in CB3 and in CB1 cells, respectively, by using electron microscopy. In cells that were incubated with NDF-gold particles at 4 °C, NDF was distributed almost exclusively on the plasma membrane, and it displayed either homogeneous distribution or local clusters (Fig. 6*A*). Within 5 min of transfer to 37 °C, most of the membrane-localized NDF disappeared, but the labeled ligand could be detected in relatively small vesicles, corresponding to early endosomes, that were located throughout the cytoplasm (Fig. 6*B*). Upon longer incubation (50 min) of cells at the elevated temperature, NDF became associated with larger elongated vesicular structures with a perinuclear location. The irregular morphology of these vesicles and the vesicular content of some structures (Fig. 6*C*, *inset*) suggest they are multivesicular bodies. By contrast, at this time point colloidal gold-labeled EGF was observed mainly in relatively large and uniform vesicles with electron dense content, consistent with their identification as lysosomes (Fig. 6*D*). Surprisingly, at this time point, gold-labeled NDF reappeared at the plasma membrane (Fig. 6*C*). Similar reappearance was not observed in the case of gold-labeled EGF, and quantitative analysis of the number of membrane-associated grains in comparison with earlier time points indicated it was statistically significant ($p < 0.023$). The reappearance of NDF at the plasma membrane probably reflects recycling of ligand-receptor complexes, or the formation of new complexes between the extracellular NDF-gold and newly maturing or recycled receptors. This conclusion is consistent with biochemical indications of ErbB-3 recycling and rapid recovery (Figs. 2 and 3). Taken together, the results presented in Fig. 6 provide structural support to the proposition based upon biochemical assays (Figs. 1 and 5) that NDF undergoes endocytosis and its degradation occurs relatively late in the endocytic pathway, namely in nonlysosomal multivesicular bodies (see also Fig. 5).

Mutational Analysis of ErbB-3 Endocytosis—Several alternative explanations to the slow endocytosis of ErbB-3 may be proposed. First, endocytosis may be impaired due to the defective kinase of ErbB-3 (45). However, the fact that ErbB-4, whose kinase is active, shares slow kinetics with ErbB-3 (Fig.

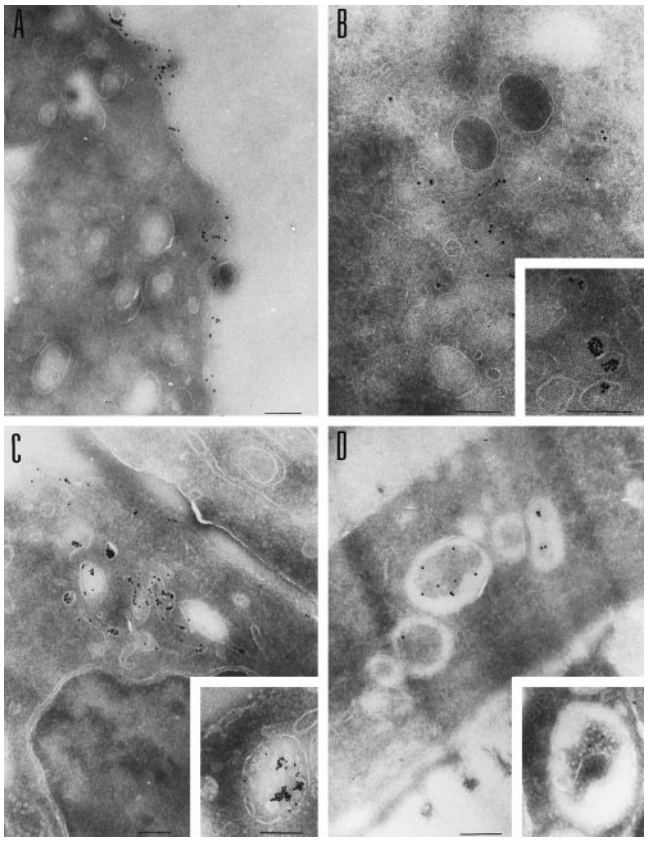

FIG. 6. **Morphological analysis of ligand internalization.** Colloidal gold-conjugated NDF or EGF was incubated for 45 min at 4 °C with CB3 (*A–C*), or CB1 cells (*D*), respectively (*bar*, 0.2 μm). *A*, following fixation, cryosections were prepared and analyzed by electron microscopy. Note the homogeneous cell surface distribution of NDF at this time point. *B*, cells were transferred to 37 °C, and after 5 min of incubation they were processed for electron microscopy. Note the appearance of NDF in small endosomes (*inset*) at this time point. *C*, cells were treated as in *B*, except that incubation at 37 °C lasted 50 min. At this time, NDF was localized to both large multivesicular endosomes (*inset*) and to the plasma membrane. *D*, CB1 cells were treated for 45 min at 4 °C with colloidal gold-conjugated EGF (10-nm particles) and then transferred to 37 °C. Following 50 min at the elevated temperature, EGF was localized to large vesicular bodies that resemble lysosomes (*inset*).

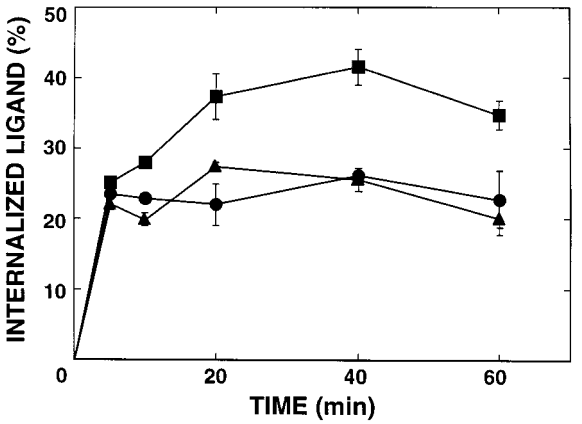

FIG. 7. **Internalization of NDF by mutant ErbB-3 proteins.** CHO cells transiently expressing wild type ErbB-3 (*circles*) or mutants that either carry a QQGFF sequence motif at the most C-terminal tail (*triangles*) or a mutant whose whole cytoplasmic domain is deleted (TAG3-M, *squares*) were grown in 24-well plates. Upon reaching 80% confluence, cells were incubated for 2 h at 4 °C with ^{125}I-NDF (10 ng/ml) and then transferred to 37 °C for the indicated periods of time. At the end of incubation, cells were rinsed twice with binding buffer, and surface-bound ligand was stripped by using a low pH solution. Intracellular radioactivity was determined and expressed as percentage of total cell-associated radioactivity at the end of incubation at 4 °C. Results shown are averages and ranges (*bars*) of duplicates. The experiment was repeated at least twice with each mutant.

1) does not support this explanation. Alternatively, because ErbB-3 does not interact with adaptor protein 2 (AP-2) of the clathrin-coated pit, but ErbB-1 efficiently associates with AP-2 (22), endocytosis of ErbB-1 is more rapid. According to a third model, an endocytosis-directing sequence motif, namely the QQGFF signal (46), which is found on ErbB-1 but not on ErbB-3, accounts for rapid endocytosis of ErbB-1. To experimentally examine this model, we constructed and transiently expressed two mutants of ErbB-3: a deletion mutant lacking the whole intracellular domain (denoted TAG-3M; Ref. 25) and a full-length ErbB-3 containing an ectopic QQGFF sequence at its C terminus (QQGFF-ErbB-3). Fig. 7 depicts the results of an NDF internalization assay performed with cells expressing the two mutants, or wild type ErbB-3. Evidently, introduction of the endocytic signal of ErbB-1 into ErbB-3 did not alter the rate of endocytosis of this NDF receptor, suggesting that the reason for the slow endocytosis may not be the absence of the QQGFF motif in ErbB-3. Likewise, deletion of the entire cytoplasmic portion of ErbB-3 only slightly affected the rate of NDF endocytosis but enhanced the overall extent of ligand internalization. Thus, it seems that a cytoplasmic sequence(s) of ErbB-3 can retard internalization, but its inhibitory action cannot be released by a sequence code containing a β-turn configuration necessary for rapid endocytosis.

The Relative Biological Potencies of ErbB Ligands Correlate with Their Endocytic Fates—The emerging differential trafficking of ligand-receptor complexes, and especially the relatively limited receptor down-regulation observed after cell stimulation with either NDF or TGF-α, prompted us to determine the implications to biological activities. Because CHO cells exhibit some characteristics of transformed cells, including tumor formation in athymic mice, we used as a cellular system an interleukin 3-dependent 32D myeloid cell line that allows sensitive detection of growth signals. Importantly, 32D cells share with CHO cells differential endocytosis of NDF and EGF receptors, including features like ligand and receptor degradation, receptor down-regulation, and recovery of binding sites after exposure to the respective ligand (Ref. 8 and data not shown). A derivative 32D line, denoted D13, that co-expresses ErbB-1 and ErbB-3 was stimulated with NDF, TGF-α, or EGF, and cell proliferation tested by using the MTT assay (30). The resulting dose-response curves indicated that NDF is the most potent of the three ligands, whereas EGF, whose effect on receptor down-regulation was most prominent (Fig. 2), is the least active mitogen in this model cell system (Fig. 8*A*). To correlate these results with possible kinetic differences in cell activation, we examined the respective patterns of receptor phosphorylation by using antibodies to phosphotyrosine (Fig. 8*B*). In experiments that are not presented, we found that mostly ErbB-3 was phosphorylated in response to NDF, and both EGF and TGF-α induced exclusive phosphorylation of ErbB-1. Likewise, MAP kinase activation was tested by utilizing an antibody specific to the active form of Erk (24) (Fig. 8*C*). Evidently, all three ligands rapidly activated receptor phosphorylation, but unlike the relatively weak activation observed with EGF, potent and persistent stimulation was displayed by both NDF and TGF-α. Surprisingly, MAP kinase activation by NDF occurred after a lag period of 1–2 min, but activation, especially of the p44 isoform of Erk, was more prolonged relative to EGF. TGF-α evoked an intermediate pattern of MAP kinase activation, consistent with its moderately high effect on cell proliferation (Fig. 8*A*). Conceivably, the combination of slow endocytosis with limited down-regulation and extensive recycling of ErbB-3 pro-

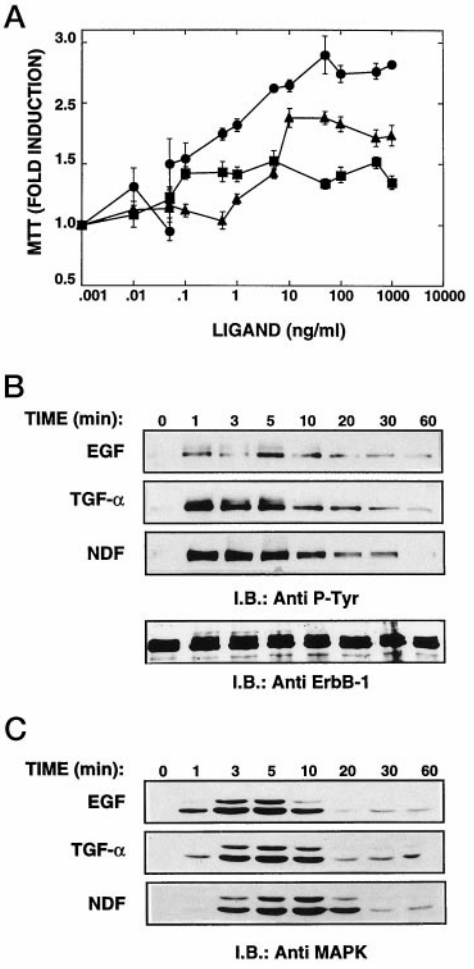

FIG. 8. **Comparative analysis of signaling potencies of NDF, TGF-α, and EGF in a model cellular system.** *A*, interleukin-3-dependent 32D myeloid cells that co-express ErbB-1 and ErbB-3 (D13 cells) were incubated at 37 °C with increasing concentrations of the following ligands: NDF (*circles*), EGF (*squares*), or TGF-α (*triangles*). Following 24 h with the ligands, the extent of cell proliferation was determined by using the MTT test. The assay was performed three times in duplicates; *bars* represent the variation. *B* and *C*, D13 cells were incubated for various time intervals with the indicated growth factors (each at 100 ng/ml). In the end of the incubation period, whole cell lysates were prepared, cleared, and subjected to immunoblotting (*I.B.*) with an antibody to phosphotyrosine (*P-Tyr*), an antibody to ErbB-1, or an antibody specific to the active doubly phosphorylated form of MAP kinase. Signal detection was performed by using a chemiluminescence kit.

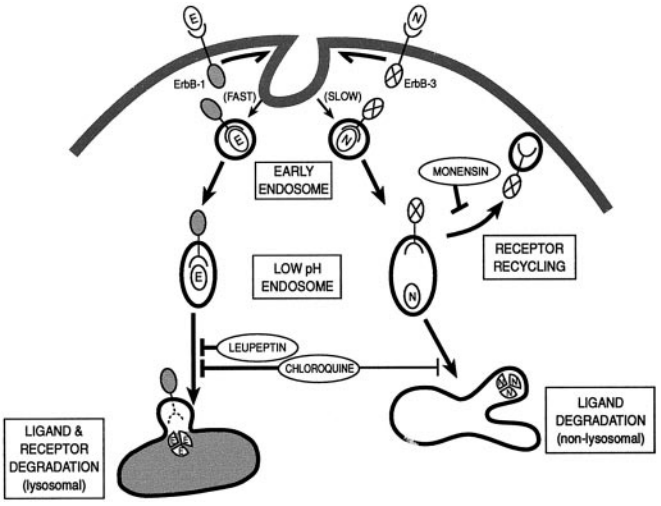

FIG. 9. **Schematic diagram of the proposed differences in cellular routing of EGF receptors and NDF receptors.** For simplicity, receptors are shown as monomers. EGF (*E*) interacts with ErbB-1, and NDF (*N*) interacts with ErbB-3. It is proposed that while the internalization induced by EGF is rapid, NDF undergoes slow uptake (see Fig. 1). Another proposed difference relates to the late endosomal stage; at the low pH characteristic to vesicles of this stage (pH 6.0–6.2), only the NDF·ErbB-3 complex dissociates, whereas the EGF·ErbB-1 complex remains intact (see Fig. 4). Therefore, whereas ErbB-3 is recycled to the cell surface, through a process that is sensitive to monensin, recycling of the EGF·ErbB-1 complex is relatively limited (see Figs. 2 and 3). As a result of these differences, EGF·ErbB-1 complexes sequester into multivesicular bodies and undergo degradation after fusion with or maturation to lysosomal vacuoles, whereas NDF does not enter the lysosomal compartment (Figs. 5 and 6). Nevertheless, NDF, like EGF, undergoes a degradative process, but this appears to take place in a nonlysosomal and leupeptin-insensitive compartment (see Fig. 5). Not represented in this model is the endocytic fate of TGF-α. Apparently, this ligand is channeled to a composite pathway; fast endocytosis by ErbB-1 is followed by dissociation of the TGF-α·ErbB-1 complex in the late endosome. Consequently, TGF-α binding to ErbB-1, like NDF binding to ErbB-3, leads to receptor recycling to the cell surface, in contrast to the primarily lysosomal destination of ErbB-1 that is dictated by EGF.

longs cell activation through the NDF·ErbB-3 complex, thereby allowing more potent mitogenic signals.

DISCUSSION

The comparative biochemical and structural analyses of ligand-mediated endocytosis of ErbB-3 and ErbB-1 we have presented in this report indicate differences between the two pathways at all steps of ligand/receptor processing, including the initial internalization step at the cell surface (Figs. 1 and 2), dissociation of the complexes in an endocytic compartment (Fig. 4), receptor recycling to the plasma membrane (Figs. 2 and 3), and degradation of both the ligand (Fig. 5) and the receptor (Fig. 1). Whereas NDF and EGF are sorted into distinct pathways, TGF-α displays a composite pathway; initially it follows an EGF-characteristic route, but later it seems to enter the NDF pathway. In some respects, the routing of ErbB-3 is analogous to the one taken by a kinase-defective ErbB-1 (41, 47, 48), implying that the impaired kinase activity of ErbB-3 is responsible for the alternative routing of this receptor. However, closer inspection of the data suggests involvement of additional parameters, which are discussed below. Fig. 9 schematically depicts the inferred distinct intracellular routes of NDF and EGF, and the following discussion highlights their major attributes.

Formation of Early Endosomes—Initially, NDF binds to surface ErbB-3 molecules (Fig. 6), whose distribution is largely similar to the pattern of surface ErbB-1 that was observed with ferritin-labeled EGF molecules (49). Within minutes at 37 °C, NDF is transferred to small and relatively clear vesicles containing 1–20 NDF-receptor complexes (Fig. 6). Despite morphological similarities to EGF internalization, removal of NDF from the cell surface is much slower than the rate of EGF or TGF-α internalization (Fig. 1). Not only is ErbB-3 a slowly internalizing receptor, but also ErbB-2 and ErbB-4 differ from ErbB-1 in their rates of endocytosis (Fig. 1 and Ref. 22). Thus, entry appears to be receptor-specific rather than ligand-specific, and its rate may be independent on kinase activity. Analyses of a kinase-defective mutant of ErbB-1 indicated that its rate of internalization is smaller than that of the wild type receptor (41, 48, 50, 51). Therefore, a causative role of the intrinsic kinase function in fast endocytosis cannot be ruled out. Conceivably, a receptor-specific sorting machinery exists at an early endocytic stage. It is unknown whether or not the same mechanism also controls the basal receptor turnover rate, which is fast in the case of ErbB-3 and slow with ErbB-1 (Fig. 1). Mutational analyses of ErbB-1 have identified sequence motifs that may be responsible for differential sorting. Thus,

two motifs, QQGFF and FYRAL, found in the C terminus of ErbB-1, could effectively replace the endocytic tyrosine-containing code of the transferrin receptor (46). Tyrosine 974 of the latter motif was shown to mediate AP-2 interactions (52). Whereas several motifs in ErbB-3 meet the FYRAL predicted structure, no analog of a QQGFF motif is found in the carboxyl-terminal tail of this receptor. Grafting this motif, however, into ErbB-3 did not recover rapid endocytosis (Fig. 7). Possibly, an active kinase is essential for the function of this motif in ErbB-3, as it is in the case of ErbB-1 (46), or additional sequences are involved.

Receptor Sorting in Endosomes—Approximately 15 min after binding to ErbB-3, NDF can be detected in large tubular-vesicular endosomes located close to the nucleus (Fig. 6). EGF follows an apparently similar pathway to reach an extensive network of tubular cisternae (49, 53). Immunocytochemical evidence suggests that the vacuolar structures with tubular arms are an important site of ligand/receptor dissociation (54). However, recycling of internalized receptors also occurs before they reach the multivesicular bodies; recycling from early endosomes is even faster than recycling from multivesicular bodies (reviewed in Ref. 16). Our structural data indicate that NDF reaches multivesicular bodies, but we were unable to determine whether at this step the ligand is still complexed to ErbB-3. Nevertheless, because the endosomal pH gradually decreases along the endocytic pathway and NDF dissociates at a relatively mild acidic pH (Fig. 4), it is conceivable that recycling of ErbB-3 occurs primarily prior to the late endosomal stage of multivesicular bodies. In fact, several biochemical lines of evidence indicate that recycling of ErbB-3 is much more extensive than that of an EGF-driven ErbB-1. Thus, exposure to high NDF concentrations resulted in a relatively moderate disappearance of ErbB-3. Moreover, inhibition of recycling with monensin enhanced the extent of ErbB-3 down-regulation, but it did not affect ErbB-1 (Fig. 2). Likewise, recovery of ErbB-3 after a down-regulation pulse is rapid and exceeds the original receptor level, indicative of accelerated delivery of receptors from internal pools (Fig. 3). The reappearance of a binding-competent ErbB-3 at the cell surface was detectable also by using electron microscopy (Fig. 6*C*). The most likely explanation to the extensive recycling of ErbB-3 is the relatively acid-sensitive NDF/ErbB-3 interaction. Presumably, an intact EGF·ErbB-1 complex mediates phosphorylation of an endosomal substrate that actively directs ErbB-1 to a lysosomal destination, but inactivation of the TGF-α·ErbB-1 complex due to ligand dissociation prevents phosphorylation of the critical substrate. In the case of the NDF·ErbB-3 complex, phosphorylation may not occur either because the kinase is inactive or because NDF dissociates from ErbB-3-containing heterodimers already at an early endocytic step. This model is compatible with the correlation reported between the pH sensitivity of several ErbB-1-specific ligands and their intracellular trafficking (19). In conclusion, recycling of ErbB-3 after NDF binding is analogous to the routing of a kinase-defective mutant of ErbB-1, whose down-regulation is defective and its recycling is enhanced (41).

Ligand Degradation—Despite remarkable differences in their cellular routing, NDF, EGF, and TGF-α undergo efficient and comparable proteolytic degradation (Fig. 5). This observation is in agreement with two recent reports that observed intracellular degradation of NDF (33) and TGF-α (43). However, unlike the well characterized degradation of EGF in mature lysosomes (Fig. 6) (for a review see Ref. 16), proteolysis of NDF and TGF-α apparently takes place in a compartment distinct from the site of EGF degradation. Our results indicate that the unknown site of NDF degradation is partly sensitive to chloroquine, a drug affecting vesicle processing at a prelysosomal site (42), but resistant to the lysosome-specific drug leupeptin (Fig. 5). Similar characteristics are shared by the degradative pathway of TGF-α (see Fig. 5 and Ref. 43). Because we observed NDF in multivesicular bodies, but not in lysosomes, it is conceivable that NDF degradation occurs in a nonlysosomal endocytic compartment.

Relationships between Intracellular Routing and Signaling Potency—Several lines of evidence support the notion that receptor endocytosis attenuates mitogenic signaling by down-regulating the receptor and by depleting the ligand from the extracellular space. An endocytosis-defective receptor for EGF delivers more potent mitogenic and oncogenic signals than the wild-type ErbB-1 (20), and an EGF mutant that cannot down-regulate its receptor due to low binding affinity and sensitivity to acidic pH elicits stronger mitogenic signals than EGF and TGF-α (21). In many cellular systems, such as keratinocytes (55) and endothelial cells (56), TGF-α is a more potent ligand than EGF. This has been attributed to the impaired ability of TGF-α to induce receptor down-regulation (34). Employing an interleukin-dependent myeloid cell line, we confirmed superiority of TGF-α, relative to EGF, but found that NDF is an even better mitogen for the same type of cells (Fig. 8). Although the greater potency of NDF may be explained by a better selection of signaling proteins by the multiple docking sites of ErbB-3 (57), the analogy with TGF-α favors the possibility that the relatively slow internalization of ErbB-3 and its extensive recycling are involved in signal amplification. Presumably, retarded depletion of NDF from the medium, along with the continuous presence of ErbB-3 on the cell surface, allows prolongation of signal transduction through the MAP kinase pathway (Fig. 8*C*). Many studies performed with well defined systems suggest that prolonged activation of the MAP kinase pathway can lead to oncogenic transformation or to cellular differentiation, depending on the cellular context (10). In the case of NDF, the relatively persistent signaling by this ligand may explain its ability to act as either a differentiation factor (58) or a very potent mitogen (8, 12).

The observation that like ErbB-3, both ErbB-4, a kinase-intact NDF-receptor, and ErbB-2, which binds all EGF-like ligands with very low affinity (3), are slowly internalizing receptors (Fig. 1 and Refs. 22 and 32) indicates that these ErbB proteins employ yet other variants of the endocytic pathway. In addition, the fact that two ligands of ErbB-1, EGF and TGF-α, remarkably differ in their trafficking implies that the two isoforms of NDF, as well as the two isoforms of the related neuregulin-2 ligands of ErbB proteins (59, 60), will follow distinct trafficking tracks. Investigation of these questions, along with the emerging possibility that endocytosis allows differential accessibility of active ligand-receptor complexes to compartmentalized effector molecules (61, 62), holds the potential for explaining diversification of signal transduction by the ErbB family.

Acknowledgments—We thank Barry Ratzkin (Amgen, Thousand Oaks, CA) for the recombinant NDF preparation, Ronit Pinkas-Kramarski and Eldad Tzahar for establishment of cell lines, and Rony Seger and John Mendelsohn for monoclonal antibodies.

REFERENCES

1. van der Geer, P., Hunter, T., and Lindberg, R. A. (1994) *Annu. Rev. Cell Biol.* **10,** 251–337
2. Burden, S., and Yarden, Y. (1997) *Neuron* **18,** 847–855
3. Tzahar, E., Pinkas-Kramarski, R., Moyer, J., Klapper, L. N., Alroy, I., Levkowitz, G., Shelly, M., Henis, S., Eisenstein, M., Ratzkin, B. J., Sela, M., Andrews, G. C., and Yarden, Y. (1997) *EMBO J.* **16,** 4938–4950
4. Alroy, I., and Yarden, Y. (1997) *FEBS Lett.* **410,** 83–86
5. Soltoff, S. P., Carraway, K. L., Prigent, S. A., Gullick, W. G., and Cantley, L. C. (1994) *Mol. Cell Biol.* **14,** 3550–3558
6. Cohen, B. D., Kiener, P. K., Green, J. M., Foy, L., Fell, H. P., and Zhang, K. (1996) *J. Biol. Chem.* **271,** 30897–30903

7. Peles, E., Ben-Levy, R., Or, E., Ullrich, A., and Yarden, Y. (1991) *EMBO J.* **10,** 2077–2086
8. Pinkas-Kramarski, R., Soussan, L., Waterman, H., Levkowitz, G., Alroy, I., Klapper, L., Lavi, S., Seger, R., Ratzkin, B., Sela, M., and Yarden, Y. (1996) *EMBO J.* **15,** 2452–2467
9. Perrimon, N., and Perkins, L. A. (1997) *Cell* **89,** 13–16
10. Marshall, C. J. (1995) *Cell* **80,** 179–185
11. Karunagaran, D., Tzahar, E., Beerli, R. R., Chen, X., Graus-Porta, D., Ratzkin, B. J., Seger, R., Hynes, N. E., and Yarden, Y. (1996) *EMBO J.* **15,** 254–264
12. Riese, D. J., van Raaij, T. M., Plowman, G. D., Andrews, G. C., and Stern, D. F. (1995) *Mol. Cell Biol.* **15,** 5770–5776
13. Faure, R., Baquiran, G., Bergeron, J. J. M., and Posner, B. I. (1992) *J. Biol. Chem.* **267,** 11215–11221
14. Yoon, C. H., Lee, J., Jongeward, G. D., and Sternberg, P. W. (1995) *Science* **269,** 1102–1105
15. Levkowitz, G., Klapper, L. N., Tzahar, E., Freywald, A., Sela, M., and Yarden, Y. (1996) *Oncogene* **12,** 1117–1125
16. Sorkin, A., and Waters, C. M. (1993) *BioEssays* **15,** 375–382
17. Kornilova, E., Sorkina, T., Beguinot, L., and Sorkin, A. (1996) *J. Biol. Chem.* **271,** 30340–30346
18. Joly, M., Kazlauskas, A., and Corvera, S. (1995) *J. Biol. Chem.* **270,** 13225–13230
19. French, A. R., Tadaki, D. K., Niyogi, S. K., and Lauffenburger, D. A. (1995) *J. Biol. Chem.* **270,** 4334–4340
20. Wells, A., Welsh, J. B., Lazar, C. S., Wiley, H. S., Gill, G. N., and Rosenfeld, M. G. (1990) *Science* **247,** 962–964
21. Reddy, C. C., Niyogi, S. K., Wells, A., Wiley, H. S., and Lauffenburger, D. A. (1996) *Nat. Biotech.* **14,** 1696–1699
22. Baulida, J., Kraus, M. H., Alimandi, M., Di Fiore, P. P., and Carpenter, G. (1996) *J. Biol. Chem.* **271,** 5251–5257
23. Chen, X., Levkowitz, G., Tzahar, E., Karunagaran, D., Lavi, S., Ben-Baruch, N., Leitner, O., Ratzkin, B. J., Bacus, S. S., and Yarden, Y. (1996) *J. Biol. Chem.* **271,** 7620–7629
24. Yung, Y., Dolginov, Y., Yao, Z., Rubinfeld, H., Michael, D., Hanoch, T., Roubini, E., Lando, Z., Zharhari, D., and Seger, R. (1997) *FEBS J.* **408,** 292–296
25. Tzahar, E., Waterman, H., Chen, X., Levkowitz, G., Karunagaran, D., Lavi, S., Ratzkin, B. J., and Yarden, Y. (1996) *Mol. Cell. Biol.* **16,** 5276–5287
26. Kunkel, T. A. (1985) *Proc. Natl. Acad. Sci. U. S. A.* **82,** 488–492
27. Karasuyama, H., and Melchers, F. (1988) *Eur. J. Immunol.* **18,** 97–104
28. Yarden, Y., Gabbay, M., and Schlessinger, J. (1981) *Biochem. Biophys. Acta* **674,** 188–203
29. Tokuyasu, K. T., and Singer, J. S. (1976) *J. Cell Biol.* **71,** 894–906
30. Mosman, T. (1983) *J. Immunol. Methods* **65,** 55–63
31. Ben-Levy, R., Peles, E., Goldman-Michael, R., and Yarden, Y. (1992) *J. Biol. Chem.* **267,** 17304–17313
32. Sorkin, A., Di Fiore, P. P., and Carpenter, G. (1993) *Oncogene* **8,** 3021–3028
33. Baulida, J., and Carpenter, G. (1997) *Exp. Cell Res.* **232,** 167–172
34. Ebner, R., and Derynck, R. (1991) *Cell Regul.* **2,** 599–612
35. Basu, S. K., Goldstein, J. L., Anderson, R. G. W., and Brown, M. S. (1981) *Cell* **24,** 493–502
36. Kramer, R. H., Leferink, A. E. G., van Bueren-Koornneef, I. L., van der Meer, A., van de Poll, M. L. M., and van Zoelen, E. J. J. (1994) *J. Biol. Chem.* **269,** 8708–8711
37. Prigent, S. A., Lemoine, N. R., Hughes, C. M., Plowman, G. D., Selden, C., and Gullick, W. J. (1992) *Oncogene* **7,** 1273–1278
38. Davis, C. G., Goldstein, J. L., Sudhof, T. C., Anderson, R. G. W., Russell, D. W., and Brown, M. S. (1987) *Nature* **326,** 760–765
39. Kadowaki, H., Kadowaki, T., Cama, A., Marcus-Samuels, B., Rovira, A., Bevins, C. L., and Taylor, S. I. (1990) *J. Biol. Chem.* **265,** 21285–21296
40. Mellman, I., Fuchs, R., and Helenius, A. (1986) *Annu. Rev. Biochem.* **55,** 663–700
41. Felder, S., Miller, K., Moehren, G., Ullrich, A., Schlessinger, J., and Hopkins, C. R. (1990) *Cell* **61,** 623–634
42. Cardelli, J. A., Richardson, J., and Meiars, D. (1989) *J. Biol. Chem.* **264,** 3454–3464
43. Hamel, F. G., Siford, G. L., Jones, J., and Duckworth, W. C. (1997) *Mol. Cell. Endocrinol.* **126,** 185–192
44. Miller, K., Beardmore, J., Kanety, H., Schlessinger, J., and Hopkins, C. R. (1986) *J. Cell Biol.* **102,** 500–509
45. Guy, P. M., Platko, J. V., Cantley, L. C., Cerione, R. A., and Carraway, K. L. (1994) *Proc. Natl. Acad. Sci. U. S. A.* **91,** 8132–8136
46. Chang, C.-P., Lazar, C. S., Walsh, B. J., Komuro, M., Collawn, J. F., Kuhn, L. A., Tainer, J. A., Trowbridge, I. S., Farquhar, M. G., Rosenfeld, M. G., Wiley, H. S., and Gill, G. N. (1993) *J. Biol. Chem.* **268,** 19312–19320
47. Chen, W. S., Lazar, C. S., Lund, K. A., Welsh, J. B., Chang, C.-P., Walton, G. M., der, C. J., Wiley, H. S., Gill, G. N., and Rosenfeld, M. G. (1989) *Cell* **59,** 33–43
48. Honegger, A. M., Dull, J. T., Felder, S., Obberghen, V. E., Bellot, F., Szapary, D., Schmidt, A., Ullrich, A., and Schlessinger, J. (1987) *Cell* **51,** 199–209
49. Haigler, H. T., McKanna, J. A., and Cohen, S. (1979) *J. Cell Biol.* **81,** 382–395
50. Glenney, J. R., Chen, W. S., Lazar, C. S., Walton, G. M., Zokas, L. M., Rosenfeld, M. G., and Gill, G. N. (1988) *Cell* **52,** 675–684
51. Sorkin, A., Helin, K., Waters, C. M., Carpenter, G., and Beguinot, L. (1992) *J. Biol. Chem.* **267,** 8672–8678
52. Sorkin, A., Mazzotti, M., Sorkina, T., Scotto, L., and Beguinot, L. (1996) *J. Biol. Chem.* **271,** 13377–13384
53. Hopkins, C. R., Gibson, A., Shipman, M., and Miller, K. (1990) *Nature* **346,** 335–339
54. Geuze, H. (1983) *Cell* **32,** 277–287
55. Barrandon, Y., and Green, H. (1987) *Cell* **50,** 1131–1137
56. Schreiber, A. B., Winkler, M. E., and Derynck, R. (1986) *Science* **232,** 1250–1253
57. Carraway, K. L., and Cantley, L. C. (1994) *Cell* **78,** 5–8
58. Bacus, S. S., Gudkov, A. V., Zelnick, C. R., Chin, D., Stern, R., Stancovski, I., Peles, E., Ben-Baruch, N., Farbstein, H., Lupu, R., Wen, D., Sela, M., and Yarden, Y. (1993) *Cancer Res.* **53,** 5251–5261
59. Carraway, K. L., III, Weber, J. L., Unger, M. J., Ledesma, J., Yu, N., and Gassman, M. (1997) *Nature* **387,** 512–516
60. Chang, H., Riese, D., Gilbert, W., Stern, D. F., and McMahan, U. J. (1997) *Nature* **387,** 509–512
61. Vieira, A. V., Lamaze, C., and Schmid, S. L. (1996) *Science* **274,** 2086–2088
62. Di Guglielmo, G. M., Baass, P. C., Ou, W.-J., Posner, B. I., and Bergeron, J. J. M. (1994) *EMBO J.* **13,** 4269–4277